ROTOR DESIGN CONSIDERATIONS TO PREVENT IMPELLER AND PREMATURE BEARING FAILURES IN CENTRIFUGAL FANS

Robert J. Sayer, PE
The Vibration Institute
2625 Butterfield Road, Suite 128N
Oak Brook, IL 60523

Abstract: Centrifugal Fans are subjected to blade-pass pulsation and mass imbalance forces as part of normal operation. Fan impellers have several n-nodal diameter modes of natural frequency that can be sensitive to blade-pass pulsation forces. Excitation of these modes can lead to catastrophic failure. The principal flexural mode of a fan rotor is sensitive to mass imbalance force, and if excited, can result in amplified stresses in the shaft and amplified force transmission to the bearings. In the case of SWSI fan rotors, where the 1-nodal diameter mode of the impeller couples with the flexural mode of the shaft, excitation of the rotor mode can lead to catastrophic failure of the impeller.

Key Words: Blade-pass pressure pulsation, centrifugal fan, critical speed, fan rotor, fan wheel, finite element analysis (FEA), natural frequency, mode shapes, nodal diameter modes, rotor dynamics.

Introduction: Fans are used for a wide variety of industrial and commercial applications. There are two primary types of fans, centrifugal (sometimes referred to as radial) and axial. This paper concentrates on the structural dynamics of centrifugal fans. A centrifugal fan system consists of a rotor (fan wheel and shaft), stationary components (fan housing, scroll, inlet cone, dampers, pedestals and foundations) and interface components (bearings).

There are two basic types of centrifugal fans. The first type is called a double-wide, double-inlet (DWDI) fan. A picture of a large DWDI fan rotor is shown in Figure 1. It consists of a shaft and a fan wheel. The fan wheel is typically mounted at the mid-span of the shaft, an equal distance from each bearing. Because the fan wheel is located at mid-span, its stiffness does not contribute significantly to the rotor dynamic properties. However, its mass is a significant factor in the rotor dynamic properties.

The second type of centrifugal fan is the single-wide, single-inlet (SWSI) fan. The location of the fan wheel on the shaft can vary for this type of fan. It can be cantilevered outside of the bearings, or located between the bearings as shown in Figure 2. In either case, the center-of-gravity of the fan wheel is not located at mid-span of the shaft, a condition which complicates the rotor dynamics thereof.

Figure 1: Photograph of a DWDI Fan Rotor Hanging in Slings

Figure 2: Photograph of a SWSI Fan Rotor Hanging in Slings

Air enters the DWDI fan wheel from both sides, flowing radially from the center of the fan to the trailing edge of the blades. Air enters the SWSI fan wheel from only one side. Dynamic forces produced by centrifugal fans as part of normal operation include imbalance forces and blade-pass pulsation forces. Fan rotors must be designed to operate subjected to these dynamic forces.

The natural frequencies of the fan wheel can be very sensitive to dynamic pressure pulsations produced either as a part of normal operation or by unusual aerodynamic circumstances. Catastrophic failures have been attributed to the excitation of natural frequencies of fan wheels by dynamic pressure pulsations (Figure 3).

Figure 3: Examples of Fan Wheel Failures Attributed to BPPF Pulsations

Blade Pass Pressure Pulsations: All fans produce dynamic pressure pulsations as the blade tip passes by the cutoff point in the housing scroll. Figure 4 shows a cross section of a housing scroll. The outer diameter of the fan is indicated as a dotted line. The fan in this illustration would be rotating in a counterclockwise direction. Air would exit the fan wheel radially into the housing and flow along the scroll until it exits the housing at the upper left quadrant.

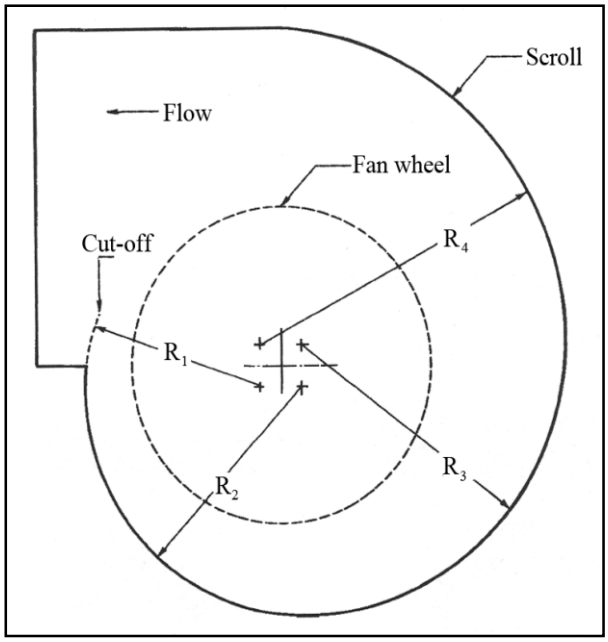

Figure 4: Cross Section of Housing Scroll

The distance between the outer diameter of the fan and the scroll gradually increases from the cut-off point to the discharge. When a blade rotates past the cutoff point, it develops a force that produces a dynamic pressure pulsation. The blade pass pulsation frequency (BPPF) is equal to the rotational speed of the fan multiplied by the number of blades. For example, a 10-bladed fan rotating at 1200 rpm would produce dynamic pressure pulsations at 12,000 cpm or 200 Hz.

Blade pass pulsations can be detected by spectral analysis of dynamic pressure data. Testing for blade pass pressure pulsations is easily done by installing a dynamic pressure transducer into the sidewall of the housing or duct. The response of the housing or duct to blade pass pulsations can also be detected with an accelerometer placed on the surface of the housing or duct.

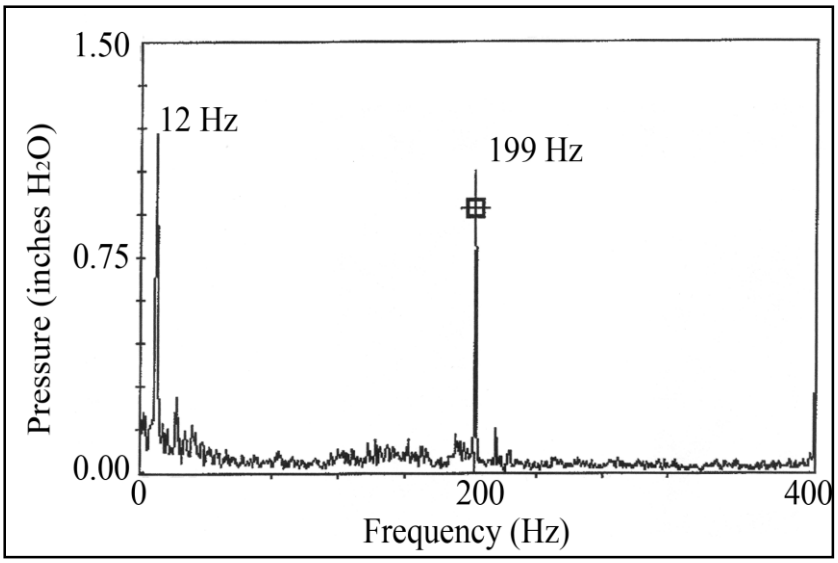

Figure 5: Frequency Spectrum of Pressure Pulsations

Figure 5 contains a spectrum of data acquired from a large 10-bladed induced-draft (ID) fan operating at 1195 rpm (19.9 Hz) using a piezoelectric dynamic pressure transducer. A spectral peak is clearly evident at the blade-pass pulsation frequency (199.0 Hz). The magnitude of the dynamic pressure developed from the BPPF was around 1.0 inches H_2O. The magnitude of this dynamic pressure is very small and is not typically large enough to damage a fan wheel. However, if the frequency of the dynamic pressure is near a natural frequency of a fan wheel, resonant amplification of stresses can cause failure. The mode of the natural frequency must be sympathetic to the BPPF force in order for resonance to be a problem.

An understanding of the modes of natural frequency of a fan wheel is imperative in order to assess the potential severity of resonant excitation by dynamic BPPF pressure. A finite element analysis (FEA) of a ten-bladed DWDI centrifugal fan was performed to illustrate the various modes of natural frequency of a fan wheel. The fan wheel used for this example was a type that is typically employed for large induced draft (ID) fans, similar to that shown in Figure 1.

n-Nodal Diameter Modes: All centrifugal fans have a set of modes of natural frequency that are called the n-nodal diameter modes. The general form of the mode shapes for these natural frequencies are such that the maximum deformations occur at the outer diameter of the wheel, at the trailing edge of a blade. The n-th degree of the mode represents the number of maximum deformations (nodal) points in either the positive or negative directions.

The n-nodal diameter modes can be very sensitive to dynamic pressure pulsations if the frequency of the dynamic pressures is close to the natural frequency of the wheel. Excitation of these modes can lead to the catastrophic failure of the fan wheel. These modes are especially sensitive when the n-th order of the mode is an integer factor of the number of blades in the fan wheel. For instance, the two-nodal diameter and five-nodal diameter modes would be very sensitive to blade pass pulsations produced by a ten-bladed fan. Likewise, the two-nodal diameter and four-nodal diameter modes would be very sensitive to blade pass pulsations produced by an eight-bladed fan.

Typically, only a few of the n-nodal diameter modes are present in most fans within the frequency range bounded by the blade pass pulsation frequency (BPPF). The natural frequency associated with these modes will increase with the n-th order of the mode. For example, the natural frequency of the four-nodal diameter mode will be greater than the natural frequency of the three-nodal diameter mode, which will be greater than the natural frequency of the two-nodal diameter mode.

With the exception of the nodal circle and wheel wobble modes, the participation of the shaft in any of the other n-nodal diameter modes is negligible. Since the deformation of the fan wheel is independent of the shaft, the transmission of vibration to the shaft and bearings is minimal when these natural frequencies are excited. Therefore, the excitation of these modes is difficult to detect during operation. If excited, catastrophic failure can occur with very little warning.

2-NODAL DIAMETER MODE: The two-nodal diameter mode is often referred to as the “chip” mode or “butterfly” mode since the deformed shape resembles a potato chip or butterfly. Figure 6 is an end view of the 2-nodal diameter mode for the example fan. The natural frequency was calculated at 128.5 Hz by the FEA. The mode shape is made up of a combination of axial and radial response. The radial and axial deformations of the side plates have two maximum positive and two maximum negative locations. The axial deformations of the side plates are in-phase while the radial deformations of the side plates are out-of-phase with each other.

The radial deformations dominate in wide fan wheels while the axial deformations dominate in narrow fan wheels. The 2-nodal diameter mode can be sensitive to dynamic forces applied either in the axial or radial direction and, thus, would be susceptible to

excitation by BPPF forces if the natural frequency and blade-pass frequency were to be near each other. For most DWDI fans, the separation margin between the natural frequency of the 2-nodal diameter mode and the BPPF is sufficient to preclude the resonant excitation of the mode. For the 10-bladed fan, the rotational speed would have to be reduced to around 780 rpm for the resonant excitation of this natural frequency, which was calculated at 128.5 Hz, to become an issue (BPPF = 780x10/60 = 130 Hz). Excitation of this mode is more common in variable-speed fans that operate at lower speeds.

If the natural frequency for this mode is excited, the deformation at any location in the wheel, either axial or radial, is countered by an equal and opposite deformation at another location. Because of these deformation characteristics, the inertia of this mode does not transfer to the shaft and the shaft does not participate in this mode. The 2-nodal diameter mode of a fan wheel can be excited, but not detectable by transducers at bearings. Strain gage testing is required to confirm excitation of this mode.

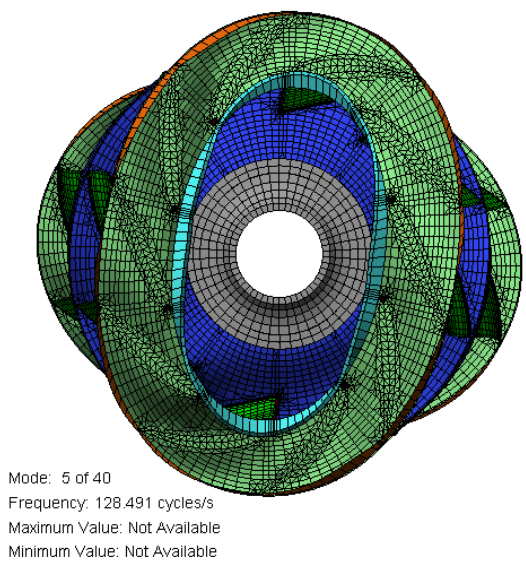

Figure 6: 2-Nodal Dia Mode

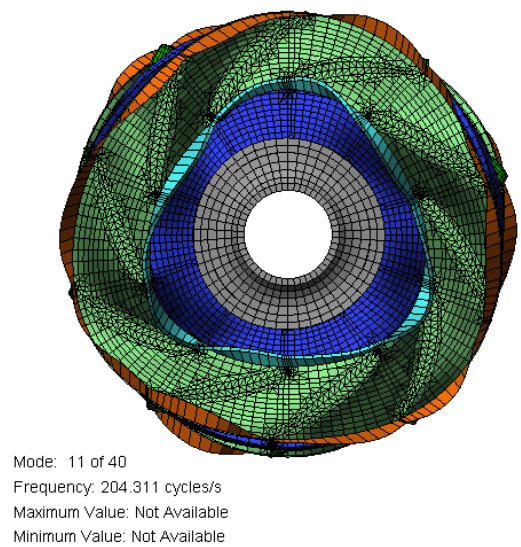

Figure 7: 3-Nodal Dia Mode

3-NODAL DIAMETER MODE: Figure 7 shows the end view of the FEA result for the 3-nodal diameter mode. This mode has both axial and radial response. The radial and axial deformations of the side plates have three maximum positive and three maximum negative locations. The axial deformations of the side plates are in-phase while the radial deformations of the side plates are out-of-phase with each other.

The natural frequency for this mode was calculated to be 204.3 Hz by the FEA . Note that this natural frequency is greater than the natural frequency of the 2-nodal diameter (128.5 Hz) mode. This is typical for all fan wheels because the complexity of the shape

increases as the order of the mode increases. It is more difficult to deform the fan wheel into a 3-lobed than a 2-lobed pattern.

The 3-nodal diameter mode can be sensitive to dynamic forces applied either in the axial or radial direction. It would be susceptible to excitation by BPPF forces if the natural frequency and blade-pass frequency were to be near each other. The 3-nodal diameter mode is more sensitive in 9-bladed and 12-bladed fans since the n-th order of the mode is an integer multiple of the number of blades (9/3 = 3 and 12/3 = 4).

For the 10-bladed fan, the BPPF would be around 200 Hz if the rotational speed of the fan were 1,200 rpm (BPPF = 1,200x10/60 = 200). In this case, the natural frequency of this fan would be in close proximity to the blade pass frequency.

Like the 2-nodal diameter mode, the deformation at any location in the wheel, either axial or radial, is countered by an equal and opposite motion at another location. Since the inertia of the wheel does not transfer to the shaft, the shaft does not participate in this mode. Even though the excitation of this natural frequency results in significant vibration within the fan wheel, it typically is not detectable by vibration probes mounted to the bearings.

4-NODAL DIAMETER MODE: Figure 8 shows the end view for the 4-nodal diameter mode. This mode also consists of a combination of both axial and radial response, each having four maximum positive and four maximum negative locations. The axial deformations of the side plates are in-phase while the radial deformations of the side plates are out-of-phase with each other.

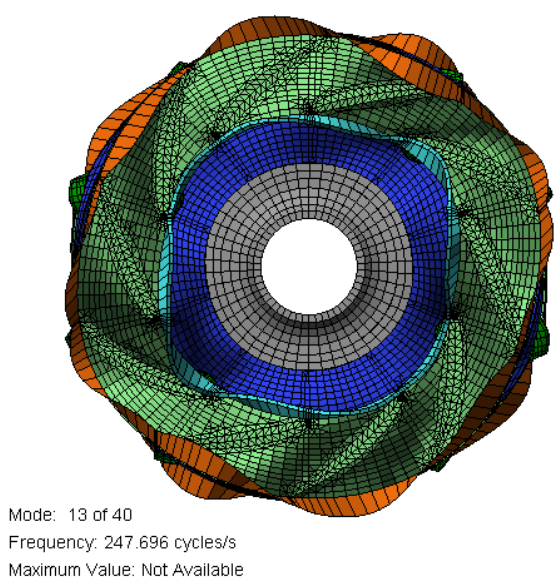

Figure 8: 4-Nodal Dia Mode

The natural frequency for this mode was estimated by the FEA as 247.6 Hz. This natural frequency is greater than the natural frequency of both the 2-nodal diameter (128.5 Hz) and 3-nodal diameter (204.3 Hz) modes.

The 4-nodal diameter mode can be sensitive to dynamic forces applied either in the axial or radial direction. The 4-nodal diameter mode is more sensitive to BPPF in 8-bladed and 12-bladed fans since the n-th order of the mode is an integer multiple of the number of blades (8/4 = 2 and 12/4 = 3).

For the 10-bladed fan, the BPPF would be around 248 Hz if the rotational speed of the fan were 1,488 rpm (BPPF = 1,488x10/60 = 248). In this case, the natural frequency of this fan would be in close proximity to the blade pass frequency.

Once again, the motion at any location in the wheel, either axial or radial, is countered by an equal and opposite motion at another location. The inertia of this mode does not transfer to the shaft. Because of this, the shaft does not participate in this mode. Since the shaft does not participate, even though the excitation of this natural frequency results in significant vibration within the fan wheel, it typically is not detectable by vibration probes mounted to the bearings.

5-NODAL DIAMETER MODE: Figure 9 shows the end view of the FEA result for the 5-nodal diameter mode. This mode has both axial and radial response. The radial and axial deformations of the side plates have five maximum positive and five maximum negative locations. The axial deformations of the side plates are in-phase while the radial deformations of the side plates are out-of-phase with each other.

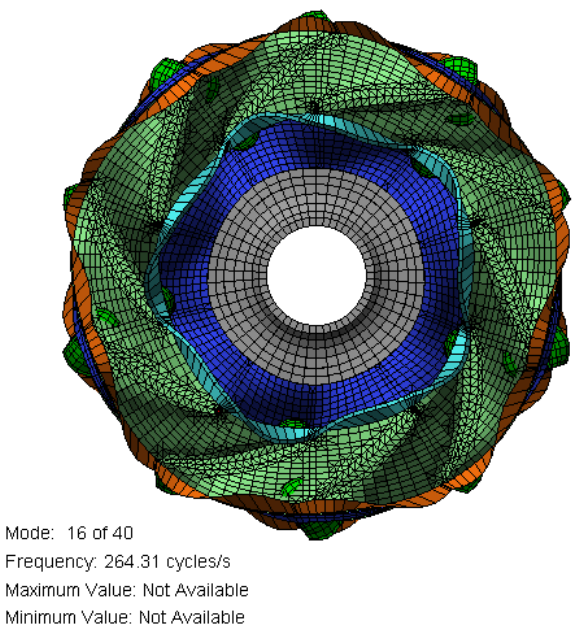

Figure 9: 5-Nodal Dia Mode

The natural frequency of this mode was calculated to be 264.3 Hz by the FEA. Note that this natural frequency is greater than the natural frequency of the 2-nodal diameter (128.5 Hz), 3-nodal diameter (204.3 Hz), and 4-nodal diameter (247.6 Hz) modes. The 5-nodal diameter mode can be sensitive to dynamic forces applied either in the axial or radial direction. The 5-nodal diameter mode is more sensitive in 10-bladed fans since the n-th order of the mode is an integer multiple of the number of blades (10/5 = 2).

For the 10-bladed fan, the BPPF would be around 264 Hz if the rotational speed of the fan were 1,584 rpm (BPPF = 1,584x10/60 = 264). In this case, the natural frequency of this fan would be in close proximity to the blade pass frequency.

Once again, the motion at any location in the wheel, either axial or radial, is countered by an equal and opposite motion at another location, the inertia of this mode does not transfer to the shaft. Because of this, the shaft does not participate in this mode. It typically is not detectable by vibration probes mounted to the bearings.

Sensitivity of n-Nodal Modes: The results of an impact test can be used to illustrate the sensitivity of the n-Nodal diameter modes of a centrifugal fan wheel. Figure 10 is the time waveform and transfer function for an impact test performed on a large induced-draft (ID) fan wheel. This test was performed with the rotor hung from flexible nylon straps, approximating a nearly free-free support condition (Figure 1).

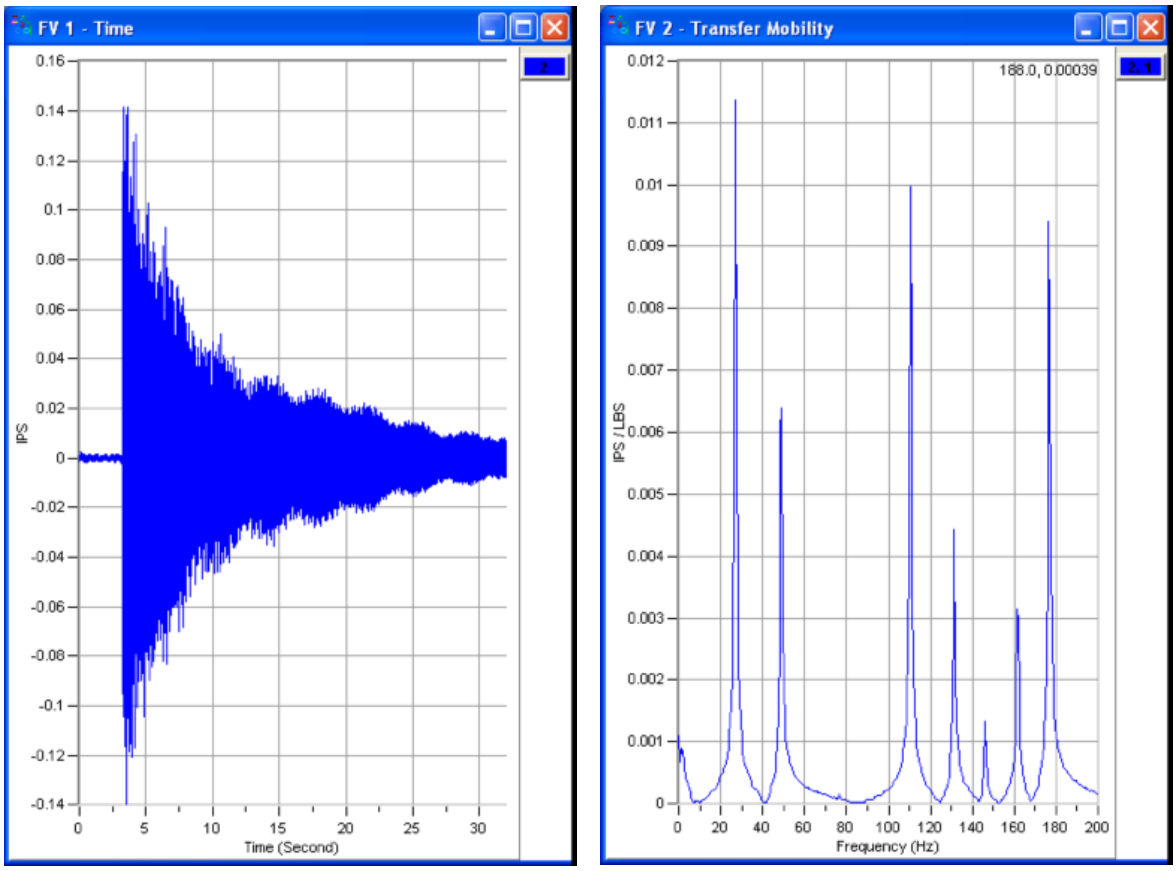

Figure 10: Waveform & Transfer Function (Natural Frequency Test of Fan Wheel)

The time waveform of the "ring-down" response shows that the fan wheel continues to vibrate over 30 seconds after application of the impact force. This is indicative of very lightly damped modes of natural frequencies. In fact, the damping factor for these modes are typically around 0.10% of critical damping ($\zeta \sim 0.001$). This low amount of damping would result in an amplification factor of around 500:1. This means that a cyclic operating stress of only 20 psi, caused by pulsation in a non-resonant fan wheel, would increase to 10,000 psi if the BPPF and the n-Nodal mode frequency would coincide.

The transfer function curve shows the many n-nodal diameter modes of the fan wheel. The narrow and steep transfer function curves also indicate lowly damped sensitive modes.

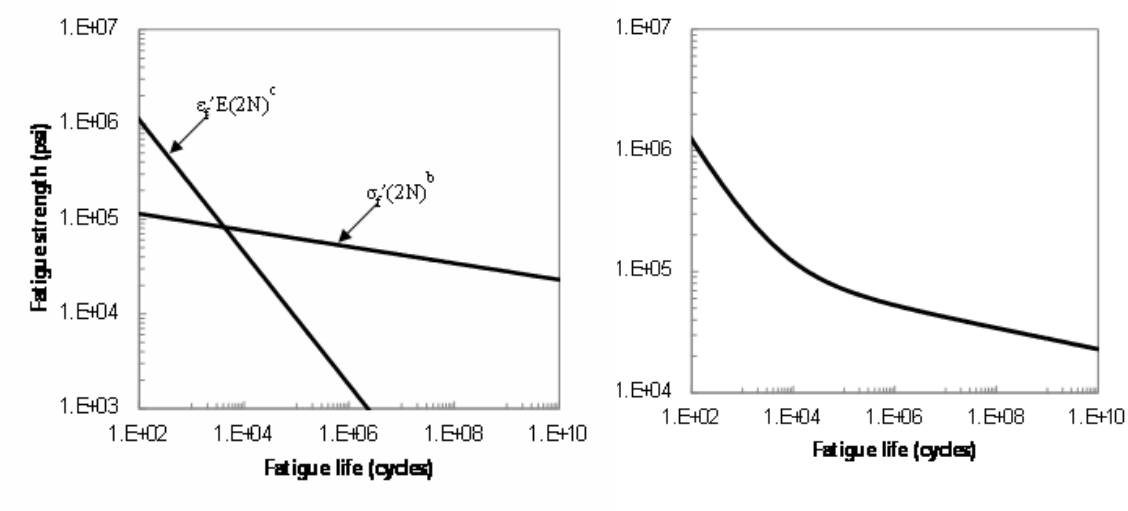

Figure 11: Notch-Strain Fatigue Life Curve

The *notch strain-life method* can be used to demonstrate the sensitivity of the n-nodal diameter modes. This method is described by a low-cycle fatigue component and a high-cycle fatigue component. Per Equation 1, the addition of these two components provides an estimate for the number of fatigue cycles to failure (2N) when subjected to a given cyclic stress ($\Delta\sigma/2$) and constant mean stress (σ_m).

$$(\Delta\sigma/2) = (\sigma_f` - \sigma_m)(2N)^b + (\varepsilon_f`)E(2N)^c \qquad \textbf{Equation 1}$$

Where $\sigma_f`$ is the fatigue strength coefficient, b is the fatigue strength exponent, $\varepsilon_f`$is the fatigue ductility coefficient, and c is the fatigue ductility exponent. References [1][2][3] are available that provide values for these coefficients and exponents for various materials.

The left side of Figure 11 contains the log-log plot of each term. When added together, these terms provide the fatigue life curve on the right side of Figure 11.

Fan wheels are subjected to numerous cycles of stress reversal in a very short time. For instance, consider a 10-bladed fan operating at 1,180 rpm. The fan wheel is subjected to 196 stress reversal per second. The accumulation of stress reversals in a single day would equal nearly 1.7 million.

For cases of high-cycle fatigue, the fatigue life equation is dominated by the first term of Equation 1 and can be simplified to Equation 2.

$$(\Delta\sigma/2) = (\sigma_f` - \sigma_m)(2N)^b \qquad \textbf{Equation 2}$$

Sensitivity Example: Consider two double-wide, double-inlet (DWDI) fan wheels of identical design, operating at 1,180 rpm (19.67 Hz). Both fan wheels have 10 blades and are subjected to pressure pulsations at blade-pass pulsation frequency (BPPF = 10 x 19.67 = 196.7 Hz). One fan experienced a fatigue failure shortly after initial start-up while the second did not experience any failures and had been operating on another unit at the same power plant for some time.

Figure 12 shows the fan rotor after the initial catastrophic failure of the first wheel. All of the blades and the side plates are missing from the wheel. This failure is consistent with the excitation of an n-nodal diameter mode of natural frequency, but since the second wheel had not failed, the failure investigation concentrated on other possible root-causes (i.e. foundation inadequacy, process parameters, acoustic amplification of pulsations, turbulence).

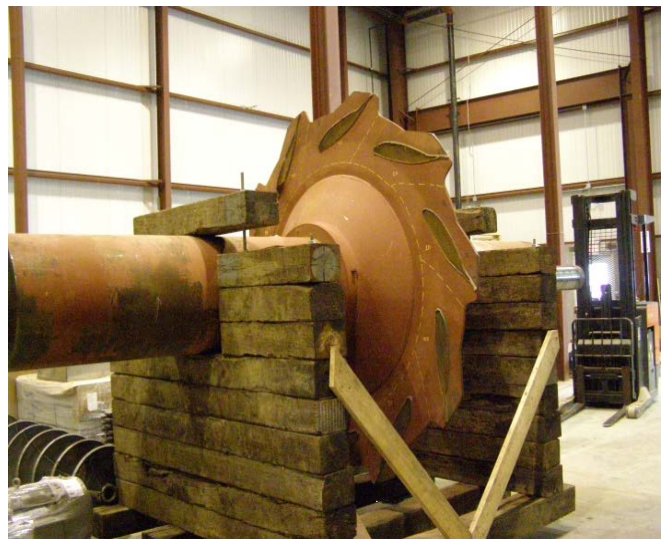

Figure 12: Fan Rotor after Wheel Failure

Modal testing and finite element analysis of the fan wheel provided an estimate of 196.0 Hz for the "stress stiffened" natural frequency associated with the 4-nodal diameter mode. Figure 8 shows the deformation shape for this mode. If excited, it results in distortion within the wheel that leads to large stresses in the welded connections between the blades and side plate. Failure of the side plates then leads to excess stresses in the welded connections between the blades and center plate, resulting in the failure pattern displayed in Figure 3 and Figure 12. If this were indeed the root-cause of the catastrophic failure, why didn't the second fan wheel fail?

The mean tensile stress developed by centrifugal forces, at the intersection of the blade tips and the side plate, was 40,000 psi for both fans. For the material used to manufacture the fans, (σ_f` = 170,000, b = -0.087) the high-cycle fatigue life equation was:

$$(\Delta\sigma/2) = (\sigma_f` - 40{,}000)(2N)^b = 130{,}000(2N)^{-0.087} \qquad \textbf{Equation 3}$$

The damping factor (ζ) for this mode was 0.003, or 0.30% of critical. This very low level of damping resulted in a very large resonant amplification factor. The ratio of the blade pass pulsation frequency to the natural frequency for the fan wheel that failed was r = 196.7/196.0 = 1.0035.

The amplification factor for resonance is given by Equation 4.

$$AF = = 1/[(1- r^2)^2 + (2\zeta r)^2]^{1/2} \quad \textbf{Equation 4}$$

Without resonance amplification, the cyclic stresses that would have been developed in the fan wheel due to BPPF were estimated at +/- 240 psi. Substituting the frequency ratio (r = 1.0025) for the fan that failed into Equation 4 yields an amplification factor of 108.4. This means that the cyclic stresses caused by the blade pass pulsations could have been as much as 26,000 psi. Substituting this cyclic stress into Equation 3 yields an estimated fatigue life of 100E06 cycles.

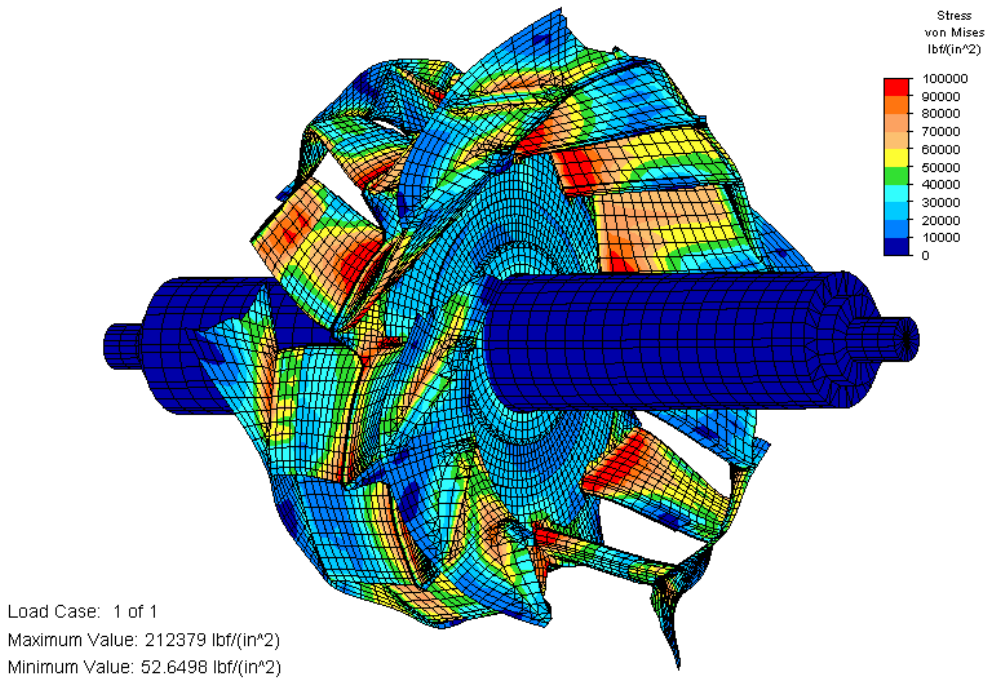

Figure 13: Final Failure Scenario after Crack Propagates Through Side Plates

The fan was subjected to 199.7 cycles of stress reversals per second, or 17.25E06 cycles per day. This means that the predicted fatigue life to crack initiation would be around 140 hours, which was consistent with the time of the actual catastrophic failure. Figure 14 is a photograph of a fan wheel that was removed from service before fatigue cracking propagated to final failure. In this case, fatigue cracks initiated in the side plate at the trailing edge of almost every blade tip.

Figure 13 is a finite element representation of the final failure scenario. Fatigue cracks that initiated at several locations on the side plates, have propagated completely through the side plates. The pieces of blades and side plates become masses cantilevered off of the center plate. Centrifugal forces acting on each cantilevered section result in high

stresses at the intersection point of the blades and center plate. The final catastrophic failure at this point is not fatigue, but overload due to the large centrifugal stress, in this case exceeding the ultimate tensile strength of the material.

Now consider that the natural frequency of the second wheel was lower than that of the first wheel by only 1.0% (f_n ~ 194.0 Hz). It is not unusual for the natural frequencies associated with the n-nodal diameter modes to differ slightly from one wheel of identical design to another. The frequency ratio for the second fan wheel increased to 1.014. Because of the steep gradient of the amplification curve, the resonant amplification factor decreased to 35.1 and resulting dynamic cyclic stress was around 8,420 psi. This seemingly small reduction in natural frequency resulted in a significant reduction in stress. The predicted fatigue life for this lower cyclic stress was 50E12 cycles, which was more than the expected useful life of the fan.

This example illustrates the sensitivity of the n-nodal diameter modes and the importance of designing a fan wheel such that these natural frequencies are not close to the blade-pass pulsation frequency.

There are other sources of pulsation that a fan can produce that are not considered as normal operating conditions, such as rotating stall pulsations and vortex shedding from dampers. These occur at frequencies other than the BPPF. It is difficult to design a fan wheel not to be resonant at these other frequencies since they are not expected to occur under normal operating conditions and their frequencies vary from fan-to-fan.

Figure 14: Fatigue Crack Initiation in Fan Wheel

Rotor Dynamics of SWSI Fan Rotor: For a DWDI fan, the wheel "wobble" mode and the shaft flexural modes will be independent of and orthogonal to each other. The modal characteristics of a SWSI fan rotor are more complex. For the SWSI fan rotor, the shaft flexural and wheel "wobble" modes will combine with each other and form two orthogonal flexural modes. Textbook formulae that treat the wheel as a lumped mass, ignoring its flexibility, cannot provide an accurate estimate of the actual natural frequency. This is illustrated in the following example.

Consider the engineering formula given in Equation 5 for the SWSI fan rotor shown in Figure 15. For this example, the fan wheel weight (W) equals 1,450 lbs., the span between bearings (L) equals 39.5 inches, the overhang distance (c) equals 14.7 inches, and the diameter of the shaft is 5 7/16 inches. The shaft is made of carbon steel (E = 29,600,000 psi).

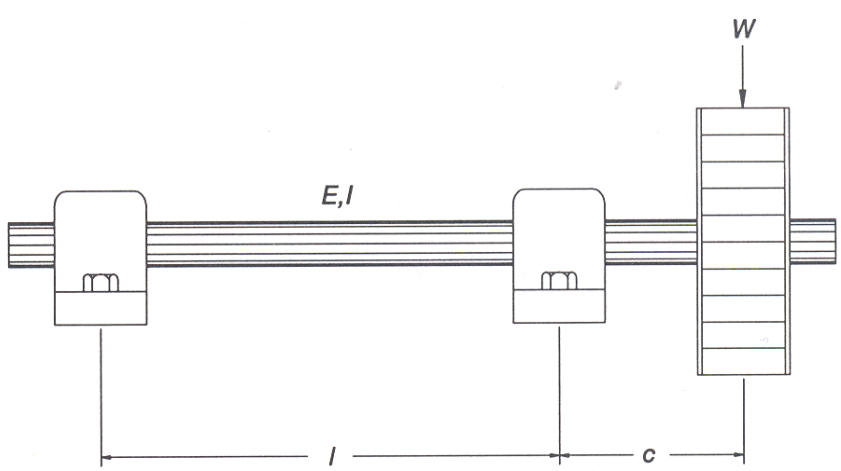

Figure 15: SWSI Fan Rotor Dimensions

Natural Frequency = $f_n = (1/2\pi)[k/M]^{1/2}$ **Equation 5**

Where: k = flexural stiffness of the shaft = $3EI/(L + c)c^2$

M = mass of the fan wheel

Substituting the known values into Equation 5, provides a calculated natural frequency of 46.4 Hz for the flexural mode of the rotor. Note that the mass of the shaft is neglected in this equation. Will the exclusion of the mass of the shaft result in an overestimation of the natural frequency? The answer is yes, but it is not the only reason that the actual natural frequency will be overestimated using the textbook formula. This equation not only neglects the mass of the shaft, assuming it to be negligible compared to that of the fan wheel, but also treats the fan wheel as a rigid component.

In reality, centrifugal fan wheels are very flexible structural components. An assumption that the fan wheel is rigid compared to the shaft is an oversimplification that will lead to erroneous results.

Figure 16: SWSI Fan Wheel

A single-wide, single-inlet (SWSI) fan wheel has blades on only one side of the back plate, and only one inlet side plate, sometimes referred to as the inlet shroud. The blades and the side plate are supported by and cantilevered off of the back plate (see photo in Figure 16). Since the back plate is a flexible structure, it results in another spring in the spring-mass system. Therefore, it cannot be treated as a single degree-of-freedom system, for which Equation 5 is only valid.

Figure 17 shows two separate spring-mass systems. Equation 5 is analogous to the lower system in the figure. There is only one spring, and it is associated with the flexural stiffness of the shaft. The mass of the fan wheel (M1) is lumped along with the mass of the shaft (M2).

The actual condition is better represented by the spring-mass system in the upper system. The lower mass represents the effective mass of the shaft. The lower spring represents the flexural stiffness of the shaft. The upper mass and spring represent the fan wheel.

Since the upper spring-mass system is a two degree-of-freedom system, it will have two natural frequencies. The motion of the masses will be in-phase with each other in the first mode of natural frequency. The motion of the masses will be out-of-phase in the second mode.

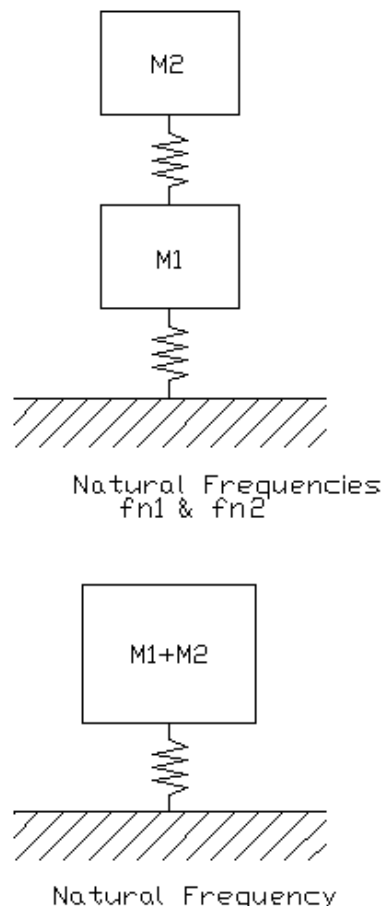

Figure 17: Spring-Mass Models

The natural frequency of the single degree-of-freedom model will be somewhere between the natural frequencies for the modes in the two degree-of-freedom system.

If f'_{n1} is the natural frequency of the single degree-of-freedom system and f_{n1} and f_{n2} are the natural frequencies of the two degree-of-freedom system, then:

$$f_{n1} < f'_{n1} < f_{n2}$$

Figure 18 shows the mode shape for a finite element analysis (FEA) of the example SWSI fan rotor. FEA [4] is a numerical technique that can account for the mass of the shaft and the flexural flexibility of the fan wheel. The mode shape in Figure 18 is for the case where the flexural displacement of the fan wheel is in-phase with the flexural displacement of the cantilevered section of the shaft. The natural frequency estimated by the FEA is 26.0 Hz, which is much less than the natural frequency (46.4 Hz) provided by Equation 5.

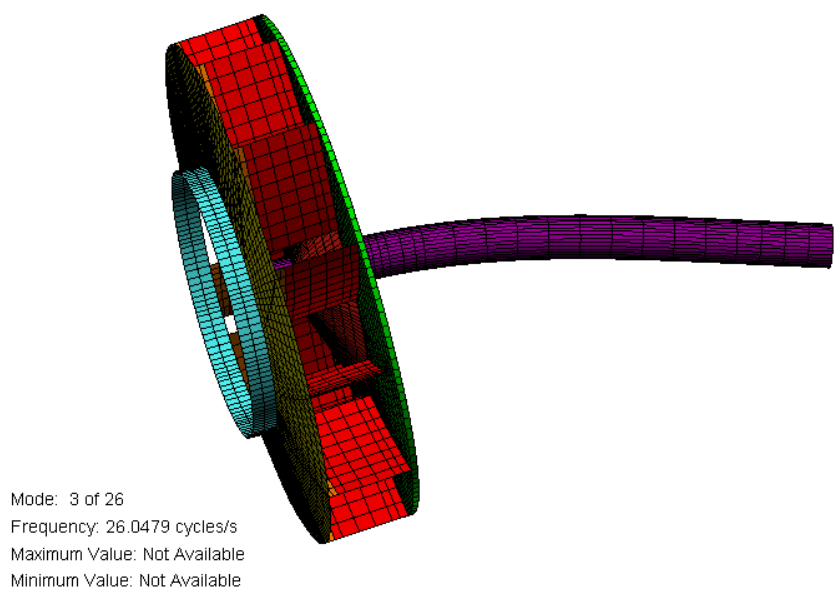

Figure 18: Mode Shape for Natural Frequency = 26.0 Hz

Figure 19 shows the mode shape for another natural frequency. This mode shape is for the case where the flexural displacement of the fan wheel is out-of-phase with the flexural displacement of the cantilevered section of the shaft. The natural frequency estimated by the FEA is 107.3 Hz, which is much greater than the natural frequency (46.4 Hz) provided by Equation 5.

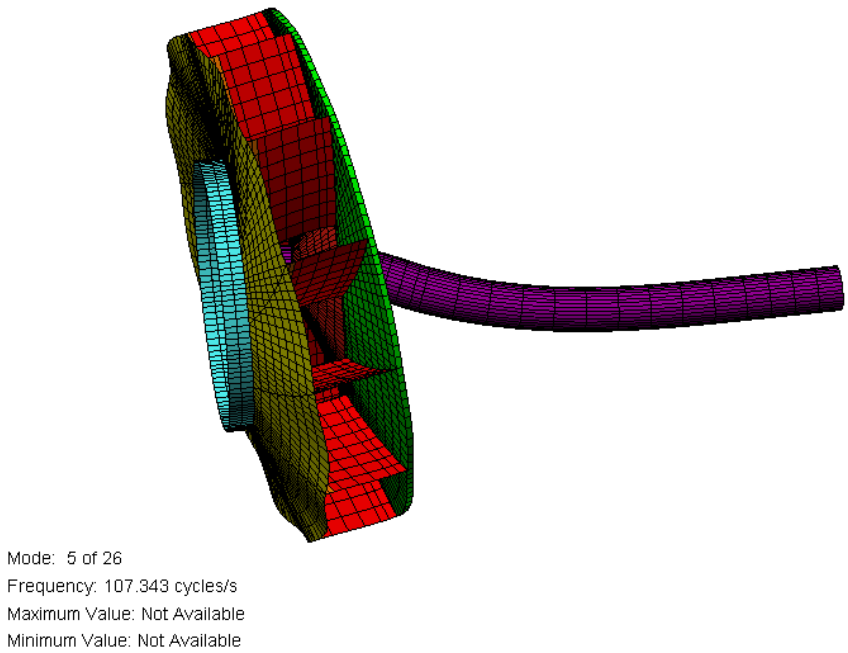

Figure 19: Mode Shape for Natural Frequency = 107.3 Hz

The significance of this analysis is that the textbook formula will always overestimate the natural frequency and provide an unrealistic estimate of the separation margin between the operating speed of the fan and its natural frequency. If the fan in the example above were to operate at 1800 rpm (30 Hz), the textbook formula provides a rather significant separation margin (f_o/f_n = 46.4/30 = 1.55). The more realistic FEA analysis would indicate a much lower separation margin (f_o/f_n = 26.0/30 = 0.87). The textbook formula indicates that the principal "at rest" natural frequency of the rotor is 55% above operating speed, while the actual "at rest" natural frequency is closer to 13% below operating speed.

Stress Stiffening: The operating natural frequencies of rotating parts of machines, such as fan wheels, pump impellers, and turbine blades, can be different from the "at rest" natural frequencies. Impact tests are performed on a rotor when it is in an idle condition. Therefore, the impact test provides the "at rest" natural frequencies of the rotor. During operation, the rotor will become stiffer due to centrifugal stresses and gyroscopic affects. Since natural frequency is a function of stiffness and mass, and the mass of the rotor is unchanged, the natural frequencies will increase as the centrifugal stress stiffening effects increase. Figure 20 displays the relationship between the natural frequency of a centrifugal fan wheel versus its operating speed. Note that since centrifugal stress increases with the square of rotational speed, the rate of increase in natural frequency is more rapid at higher speeds. The amount of increase in the natural frequency is not only dependent upon the rotational speed of the fan, but on the amount of centrifugal stress. Thus, it can vary widely from one fan design to another.

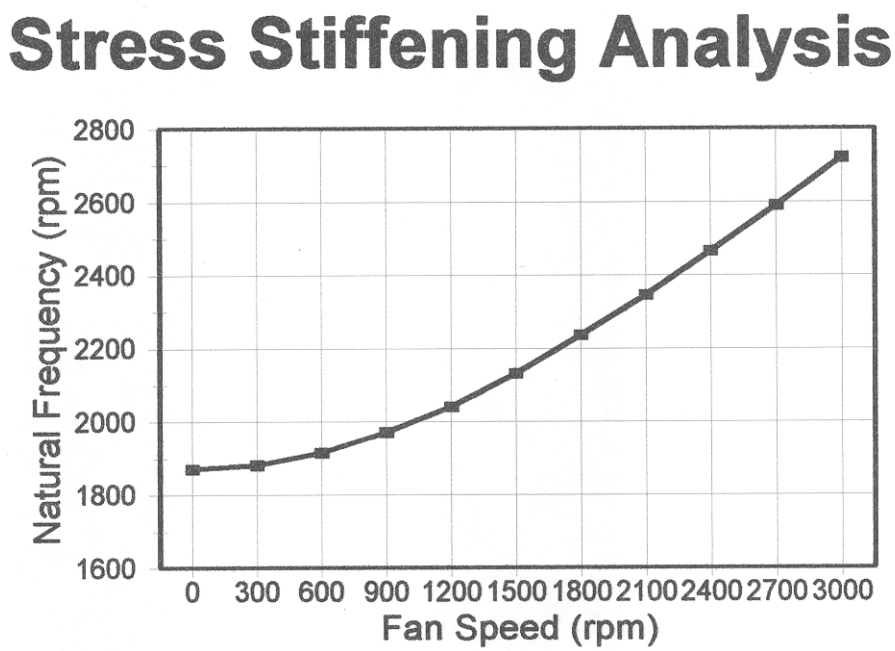

Figure 20: Stress Stiffening Curve

The importance of stress stiffening is that, if an inappropriate single dof model is used to estimate the natural frequency of a SWSI fan rotor, there is a good chance that the actual "at rest" natural frequency will be less than the operating speed of the fan. Since stress stiffening will increase the natural frequency during operation, there is a chance that the natural frequency and operating speed will be too close to each other. It is imperative that the numerical technique used to design the fan rotor provide an accurate assessment of the nature frequency.

References:

[1] J. A. Graham (Editor), *Fatigue Design Handbook*, Advances in Engineering Series (Volume 4), Society of Automotive Engineers, Warrendale, PA, 1968.

[2] R. L.Wetzel (Editor), *Fatigue under Complex Loading*, Advances in Engineering Series (Volume 6), Society of Automotive Engineers, Warrendale, PA, 1977.

[3] H. O. Fuchs and R. I. Stephens, *Metal Fatigue in Engineering*, John Wiley and Sons, New York, 1980.

[4] R. J. Sayer, *Finite Element Analysis; A Numerical Tool for Root-Cause Vibration Analysis*, Proceedings of the 27th Annual Meeting of the Vibration Institute, New Orleans, LA, July 2003.